Patterns of earthquake swarm activity

(Earthquake swarms)

S. J. Gibowicz (*)

Received on September 4th, 1973

Summary. — Examination of ten earthquake swarms in different seismotectonic settings suggest that swarms can be classified both by the pattern of variation in the frequency-magnitude relation, and by that in the rate of occurrence. The coefficient *b* varies in one of three different ways: (1) a steady increase, (2) a steady decrease, (3) a decrease followed by an increase after the largest shocks. The rate of occurrence can vary in four ways: (A) hyperbolic decay, as in an aftershock sequence; (B) as in sequence with foreshocks and aftershocks; (C) complex, with several segments of type A; (D) complex, with several segments of type B.

Riassunto. — Dopo aver esaminato 10 sciami di terremoti avvenuti lungo diverse direzioni sismotettoniche, l'A. suggerisce l'idea che questi possono essere classificati sia mediante la variazione di *b* nella relazione frequenza-magnitudo sia attraverso il ricorso degli eventi sismici. Il coefficiente *b* varia in uno dei seguenti tre modi: (1) aumento costante; (2) diminuzione costante; (3) diminuzione seguita da aumento dopo le scosse più forti. Il ricorso dell'evento sismico può variare in quattro modi: (A) decadimento iperbolico, come avviene in una serie di repliche; (B) come si verifica in una serie di scosse premonitorie e repliche; (C) complesso, comprendente parecchi tratti di tipo A; (D) complesso, comprendente parecchi tratti di tipo B.

Introduction

Earthquake swarms are commonly described as sequences of shocks closely grouped in time and space, but with no single outstanding

(*) Seismological Observatory Geophysics Division Department of Scientific and Industrial Research, Wellington, New Zealand.

event. Mogi [17], who has performed experiments on microfracturing of rocks, found that a swarm-like sequence of fractures occurs when material of very heterogeneous composition is placed under highly concentrated external stress.

Many earthquake swarms are known to occur in volcanic regions [3, 12, 18, 28, 32], which are probably regions of highly concentrated stress. They also commonly occur near the fracture zones of ocean ridges [8, 24, 27, 34]. Few swarms are reported from non-volcanic areas, or from regions where no recent volcanism is observed [16, 21, 25].

The observed pattern of aftershock sequences has been described [19, 20], but little is known about the pattern of swarm activity. Ten earthquake swarms for which sufficient data have been published (Table I) will be considered. The pattern of these swarms will be considered in terms of the frequency-magnitude relationship and of the rate of occurrence and the variation of these with time.

TABLE I – SELECTED EARTHQUAKE SWARMS

Event code	Location	Date	Reference
KMR	Kermadec Ridge	1961 Apr. 18	Gibowicz [8]
MKI	Miyake Island, Japan	1962 Aug. 25	Oike [18], JMA Bulletins
TPZ	Taupo, New Zealand	1964 Dec. 4	Gibowicz [6]
KDR	Kermadec Ridge	1965 Jan. 8	Gibowicz [8]
MBC	Mould Bay, Canada	1965 Mar. 29	Smith *et al* [23]
MSR	Matsushiro, Japan	1965 Aug. 7	Hagiwara and Iwata [10], Ichikawa [11], JMA Bulletins
QCI	Queen, Charlotte Islands, Canada	1967 Aug 27	Westmiller [34], ISC Bulletins
RPI	Reykjanes Peninsula, Iceland	1967 Sep. 28	Tryggvason [28]
GPI	Galapagos Islands	1968 Jun. 12	Iwata[12], ISC Bulletins
DVC	Danville, California	1970 May 25	Lee *et al* [16]

DATA

The main characteristics of the selected swarms are listed in Table II. The sequences lasted from 2 days to over 2 years, the magnitudes of the largest shocks were from 3 to 6, and the number of obser-

vations varies from about 200 to over 60,000. In four cases there are not sufficient data to study the frequency-magnitude variation.

The Matsushiro swarm has been extensively studied [10, 11, 14, 15] but no list of magnitudes has been published, except for the largest shocks [10]. On the other hand, the JMA Bulletins list the time of occurrence and felt intensity at Matsushiro Observatory for over 60,000 shocks. An attempt is made here to use these intensity reports to derive a frequency-magnitude relationship.

Variation of frequency-magnitude relation

The frequency-magnitude relation is commonly written

$$\log N_M = a - bM, \qquad [1]$$

where N_M is the number of earthquakes within a given magnitude interval $M \pm \Delta M/2$, and a and b are constants [9]. The numerical value of a depends upon the other terms in the expression. The constant b can be found by the maximum likelihood method of Utsu [30]

$$b = \frac{\log e}{\overline{M} - M_0}, \qquad [2]$$

where $\overline{M} = \sum_{i=1}^{N} M_i/N$ is the mean magnitude of the group of earthquakes, M_0 is the smallest magnitude considered, and N is the number of events larger than M_0. When the magnitude interval ΔM is large, further corrections to the value of b must be applied [31].

The coefficient b depends upon the proportion of large to small shocks in a given group of earthquakes. When b is large, small shocks predominate, and conversely.

Several magnitude scales were used for b determination (Table II). These scales are not identical and the b values obtained from them are not necessarily comparable, even when the scales are linearly related. This is due to the different magnitude intervals involved when different scales are used. However, values of b based on M_L and m are close enough to be directly comparable [4]. The difference between the original magnitude scale M_L and the local scales M_{JMA} and M_{REY}, although not precisely known, is believed to be small as these scales were intended to approximate to M_L values. This means that b values based on them are also approximately comparable.

Several numerical tests were applied to the list of intensities at the Matsushiro Observatory ($I_{MAT} \geqslant 1$ on the JMA intensity scale), to see whether equation [1] was valid when intensity was substituted for magnitude. These tests were applied to groups of from 2,000 to 60,000 shocks, and showed that the substitution was legitimate, but the value derived will be designated b'. Magnitude and intensity are therefore linearly related in this case, as has been found in other regions [see review by Karnik ([13])].

The slope coefficient of the magnitude-intensity relation is in most cases close to 0.6 ([13]), for intensities given on a 12 degree scale (usually the modified Mercalli scale). The JMA intensity scale contains only 7 degrees, which may imply a slope coefficient close to one. If so, $b' = b$, and direct comparison between them for the whole sequence provides further evidence that this is so. The value of b obtained from 300 earthquakes, for which Ichikawa ([11]) gives magnitudes ($M_{JMA} \geqslant 3.8$), is $b = 0.90 \pm 0.10$, which is identical with the value of $\bar{b}'$ (Table II).

The intensities reported by the JMA are those felt at the Matsushiro Observatory and not those expected at the epicentre. However, during the year for which the first two stages of the swarm lasted, the Observatory was situated near its centre, and the activity was concentrated within a circle of radius 5-6 km ([10]). For that period at least the Observatory reports may be assumed to be complete for the area involved. During later stages, in the second year, the activity spread in two directions and became elliptical. But the values of b' continue to display a regular pattern of change with time.

Values of $\bar{b}$ for the whole of each sequence are listed in Table II. The 95% confidence limits have been calculated by the method of Aki ([1]). The values lie in the range 0.6 — 1.5. Swarms from fractures zones of oceanic ridges are characterised by the values of $\bar{b}$ greater than 1. This may imply that the stress-field in these cases is primarily of thermal origin and directly related to volcanic activity, but the values observed there are not as high as those observed in thermally induced microfracturing of rocks ([33]). During the Galapagos Islands swarm, volcanic eruption occurred and collapse of the caldera floor was observed ([12]).

There is now strong evidence from the experiments on microfracturing of rocks ([22]) and from earthquakes ([7,35]) that the coefficient $\bar{b}$ is inversely correlated with the stress. During some New Zealand

TABLE II. – CHARACTERISTICS OF EARTHQUAKE SWARMS

Event code	Period of observation (days)	Magnitude scale	Largest magnitude	Smallest magnitude observed	Number of shocks	Magnitude interval	Coefficient b at 95% confidence limits	Coefficient p in final stage	Type	
									$b(t)$	$n(t)$
KMR	2.3	M_L	5.0	3.9	241	0.2	1.50 ± 0.19	-0.94	3	B
MKI [1]	38	M_{JMA}	5.9	?	1034	0.5 [3]	0.84 ± 0.21 [3]	-0.95	3?	C
TPZ	59	M_L	4.5	2.7	1126	0.1	0.82 ± 0.05	-0.96	2	C
KDR	13.5	M_L	5.6	4.0	176	0.3	1.34 ± 0.20	-0.91	2	A
MBC [1]	28	M_L	2.9	-1.1	2026	0.5	0.69 ± 0.03	-0.92	4?	D
MSR	770	I_{MAT} [2]	5	I	61000	I	0.90 ± 0.01	-1.11	3	D
QCI [1]	5.4	m	5.2	2.7	217	0.2 [4]	1.3 ± 0.2 [4]	-1.06	3?	B
RPI [1]	2.5	M_{REY}	4.9	1.7	480	0.4	0.64 ± 0.06	-1.00	2	D
GPI	20.5	m	5.4	4.2	291	0.3	1.26 ± 0.14	-1.21	1	B
DVC	46	M_L	4.3	1.1	379	0.4	0.66 ± 0.07	-1.08	1 [5]	A [5]

[1]) Published data are insufficient for study of $b(t)$.
[2]) Data and calculations are based on the JMA intensity observed at Matsushiro Observatory.
[3]) From 58 earthquakes with $M_{JMA} > 4$, published in JMA Bulletins.
[4]) From Westmiller ([31]).
[5]) This swarm seems to consist of two distinct sequences, both of type 1-A.

earthquake sequences b was found to vary. This was interpreted in terms of stress changes during the sequence ([5]).

A very simple technique, applying formula [2] to a fixed number of earthquakes N, has been used to study the variation of b during the sequence. This procedure establishes a constant statistical uncertainty and a variable time-window. The results for the six swarms are shown in Figures 1-6.

The variation of b is regular and can be approximated by

$$b = \alpha + \beta \log t, \qquad [3]$$

where t is the time from the beginning of the sequence in days, and α and β are constants ([6]). Values of β are given in Figures 1-6, and values of α can be readily found from the same figures.

Statistical significance of the difference in b-value can be tested by the F-test ([31]). The difference between the highest and the lowest values of b is statistically significant at 99% confidence level during the Taupo swarm, the Matsushiro swarm, the Galapagos Islands swarm, and the Danville swarm; at 95% during the Kermadec Ridge swarm of 1961; and at 75% during the Kermadec Ridge swarm of 1965.

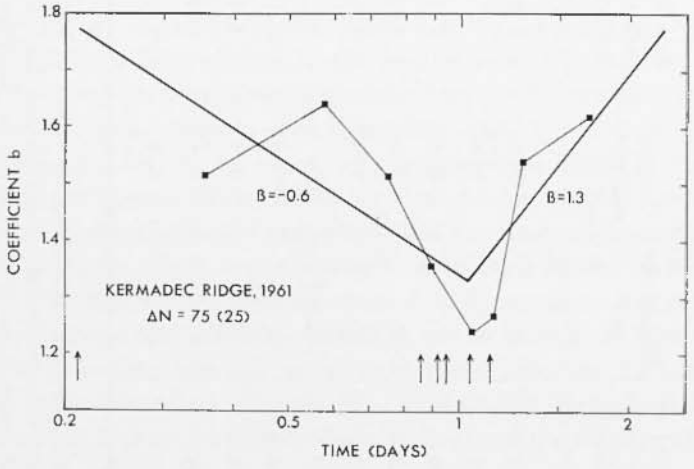

Fig. 1 – Variation of b during the Kermadec Ridge swarm of 1961. Values are calculated for a fixed number of shocks $\Delta N = 75$ at intervals of 25 shocks, and assigned to the mean of each time interval involved. The arrows show the time of occurrence of earthquake with $M_L \geqslant 4^3/_4$.

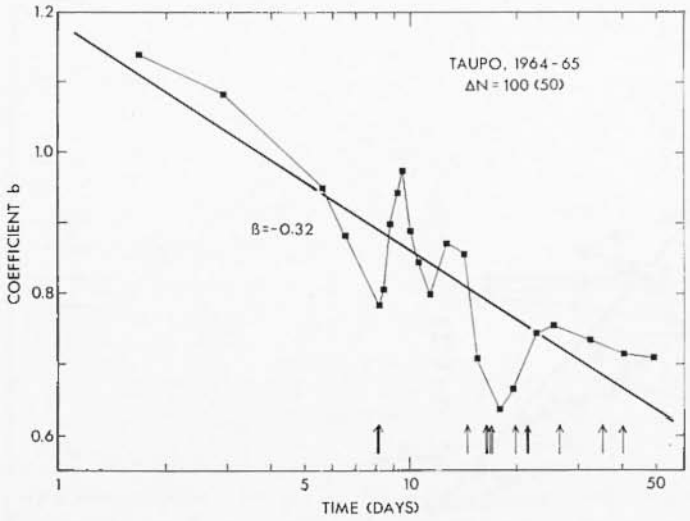

Fig. 2 – Variation of b during the Taupo swarm. Values are calculated for $\Delta N = 100$ at intervals of 50 shocks. The arrows show earthquakes with $M_L \geqslant 4.4$.

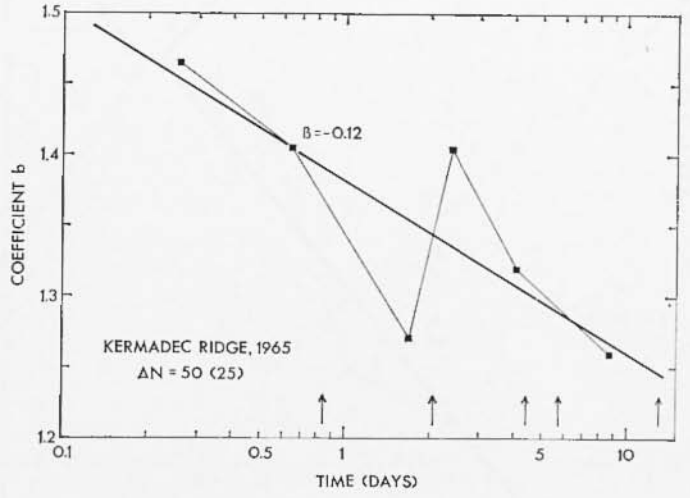

Fig. 3 – Variation of b during the Kermadec Ridge swarm of 1965. Values are calculated for $\Delta N = 50$ at intervals of 25 shocks. The arrows show earthquakes with $M_L \geqslant 5$.

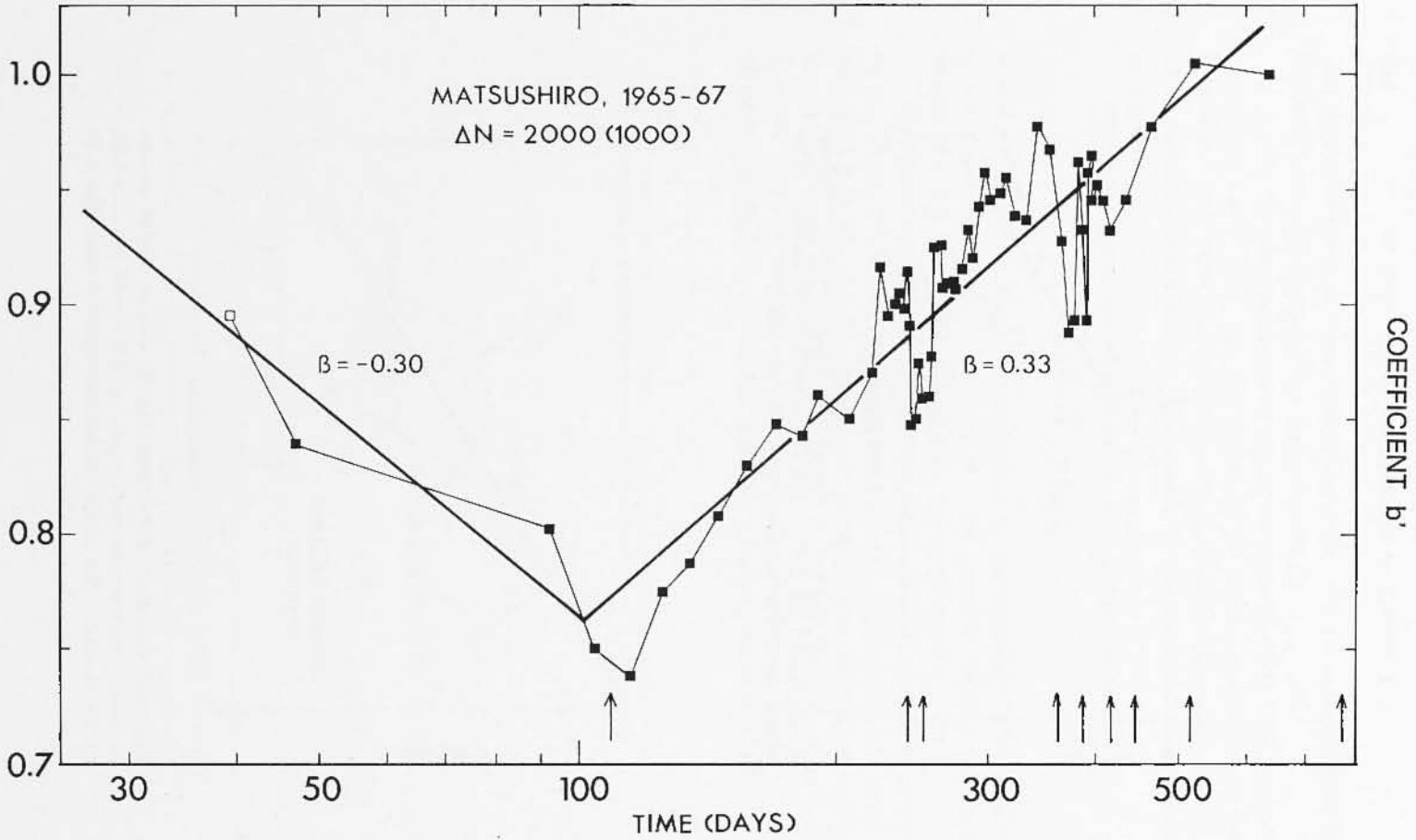

Fig. 4 – Variation of b' during the Matsushiro swarm. Values are calculated for $\Delta N = 2000$ at intervals of 1000 shocks. The initial value, shown by an open square, is for $\Delta N = 1000$. The arrows show earthquakes with $M_{JMA} \geqslant 5.0$.

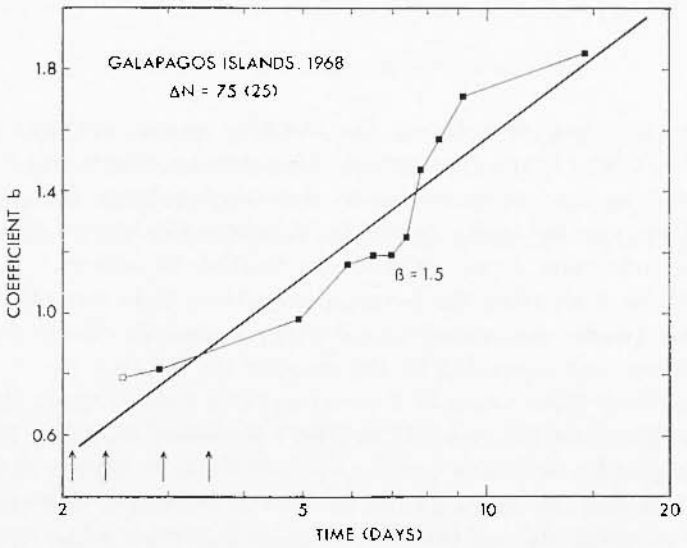

Fig. 5 – Variation of b during the Galapagos Islands swarm. Values are calculated for $\Delta N = 75$ at intervals of 25 shocks. The first value is for $\Delta N = 50$. The arrows show earthquakes with $m \geqslant 5\ ^1/_4$.

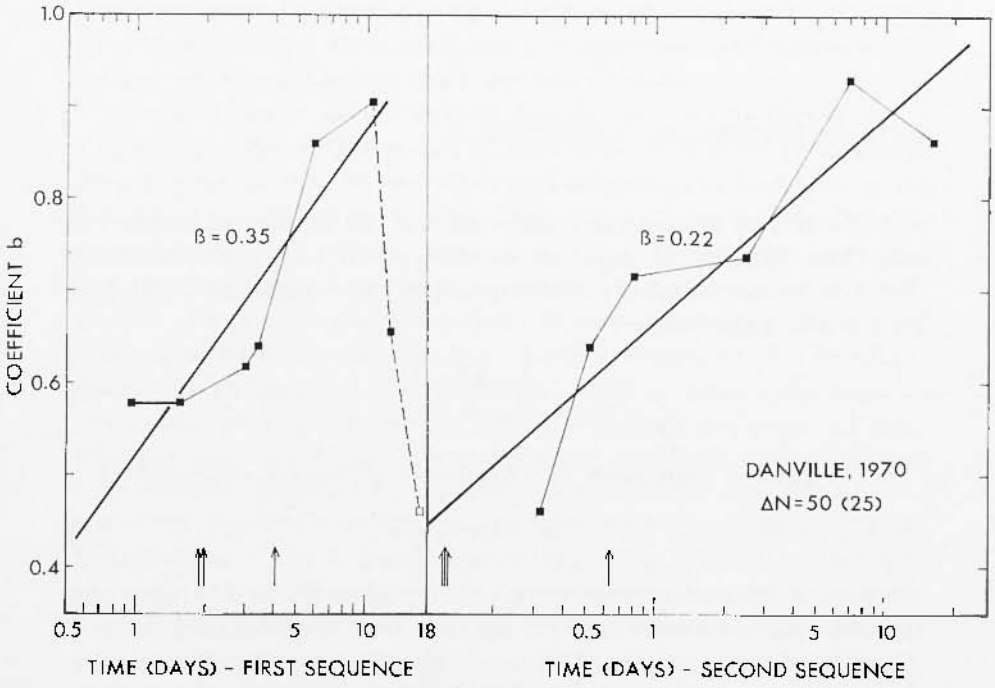

Fig. 6. – Variation of b during the Danville swarm, consisting of two distinct sequences. The vertical line marks the beginning of the second sequence. Values are calculated for $\Delta N = 50$ at intervals of 25 shocks. The two sequences are plotted on different time scales. The open square marks the value of b calculated using 25 shocks from each sequence. The arrows show earthquakes with $M_L \geqslant 3.5$.

The variation of b during the Danville swarm has been studied by Bufe [2], who found that periods of maximum elastic-strain release were preceded and accompanied by a marked decrease in b. Similar conclusions can be drawn from Fig. 6, where the largest shocks (indicating maximum strain release) are marked by arrows. It seems, however, on comparing the b–variation pattern from various swarms, that this swarm consists of two distinct sequences closely following one another, and separated by the onset of the fall in b.

There are three types of b variation with time. During the Galapagos Islands and the Danville swarms b increased smoothly from the beginning of the sequence until the swarm finished; during the Taupo and the Kermadec Ridge swarm of 1965 b decreased, and the larger shocks occurred during the final stages; and during the Kermadec Ridge swarm of 1961 and the Matsushiro swarm b decreased from the beginning until the occurrence of the largest shocks, in the middle of the swarm, and then increased until the earthquakes stopped. These patterns imply that the stress changes in the different sequences have different characters.

Rate of earthquake occurrence

The rate of earthquake occurrence n is the number of shocks per unit time (usually one day), above some given magnitude threshold. If ΔN is a fixed number of shocks, and δt the variable time interval during which they occur

$$n = \frac{\Delta N}{\delta t}. \qquad [4]$$

The rate of occurrence of aftershocks is usually expressed as

$$n = n_1 \cdot t^p, \qquad [5]$$

where n_1 is the rate of occurrence one day after the beginning of the sequence, p is a constant, and t is the time from the beginning in days. The value of p is usually close to -1, which means that the activity decays hyperbolically with time [20].

Earthquake swarms usually occur in several stages, during which the rate of occurrence increases and decreases alternately. To study this pattern a modified formula is needed. If t_o is the beginning of a given stage of the swarm, and t is the time from the beginning of the sequence,

$$n = n_1 \ (t - t_o)^p. \qquad [6]$$

The change in the rate of occurrence during ten selected earthquake swarms is shown in Figures 7-16. The values have been obtained using equation [4]. Approximations to the changes, calculated from equation [6], have been fitted by least-squares. The rates have been plotted logarithmically, but a linear scale has been used for time, so that the whole sequence can be shown on a common scale. Values of p and t_o are also given.

For the Mould Bay, Queen Charlotte Islands and Reykjanes sequences the data were given in the form of diagrams showing the frequency-time distribution. The numbers of events per unit time were obtained from these diagrams and converted into intervals containing an approximately fixed number of shocks.

Several types of earthquake swarm can be distinguished. A single stage type with the rate of occurrence decreasing in a manner very similar to that for an aftershock sequence, is seen during the Kermadec Ridge swarm of 1965 (Fig. 10) and during the Danville sequence (Fig. 16). Two stages of activity, the rate first increasing and then decreasing, are displayed during the Kermadec Ridge swarm of 1961 (Fig. 7), the Queen Charlotte Islands swarm (Fig. 13) and the Galapagos Islands swarm (Fig. 15). These are similar to the foreshock-aftershock pattern, but the "foreshock" stage is much more vigorous during the swarm, than during normal foreshock sequence. A complex pattern, containing several stages of foreshock and aftershock-type activity, occurred in the other cases. These complex patterns are of two kinds: one containing only aftershock-like segments (Miyake Island swarm – Fig. 8, and Tanpo swarm – Fig. 9) and the other with segments of both foreshock and aftershock type (Mould Bay swarm – Fig. 11, Matsushiro swarm – Fig. 12, and Reykjanes swarm – Fig. 14).

In all cases the decay coefficient p is very close to -1 during the final stage of a swarm (Table II).

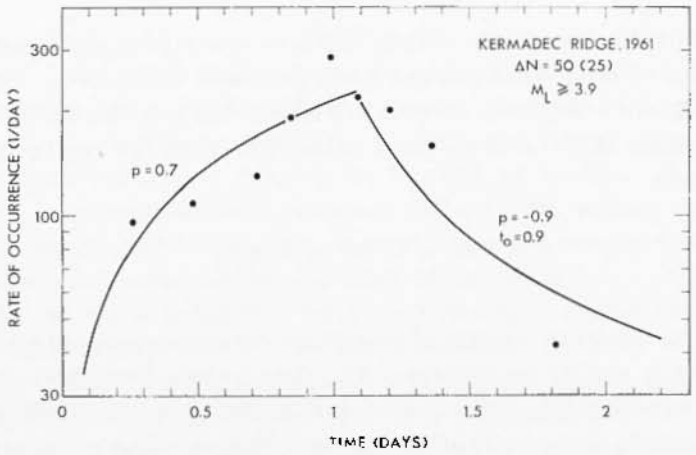

Fig. 7 – Rate of occurrence versus time, for earthquakes with $M_L \geq 3.9$, during the Kermadec Ridge swarm of 1961. Values are calculated for $\Delta N = 50$ at intervals of 25 shocks, and assigned to the mean of each time interval.

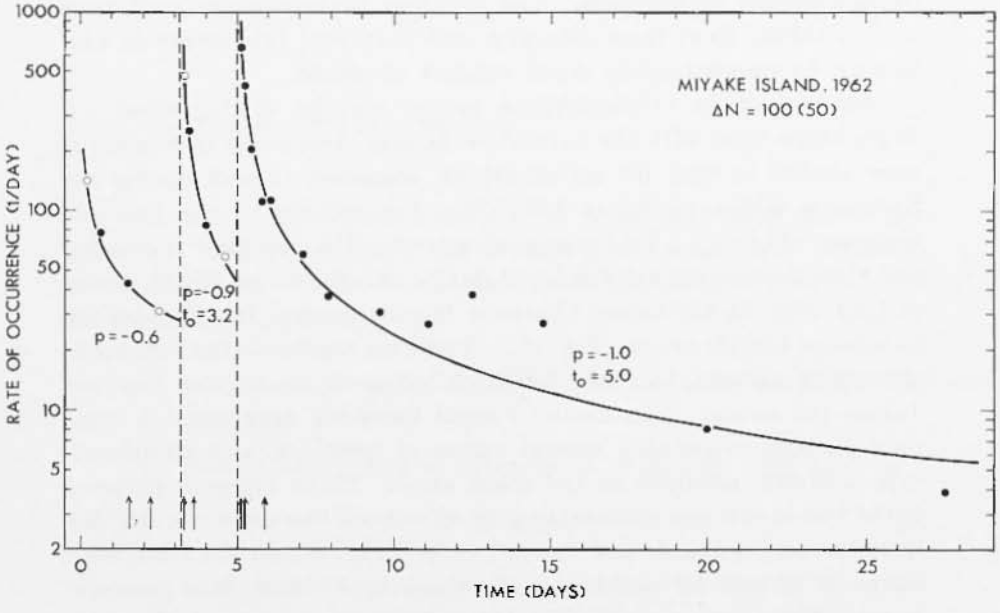

Fig. 8 – Rate of occurrence versus time during the Miyake Island swarm. Values are calculated for $\Delta N = 100$ at intervals of 50 shocks. Open circles are for $\Delta N = 50$. The broken vertical lines mark the beginnings of the second and third stages of the swarm. The arrows show earthquakes with $M_{JMA} \geq 5.2$.

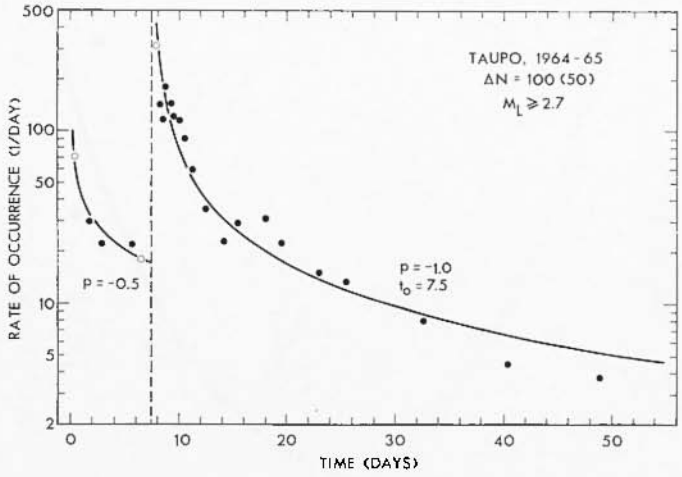

Fig. 9 – Rate of occurrence versus time, for earthquakes with $M_L \geq 2.7$, during the Taupo swarm. Values are calculated for $\Delta N = 100$ at intervals of 50 shocks. Open circles are for $\Delta N = 50$. The broken line marks the beginning of the second stage.

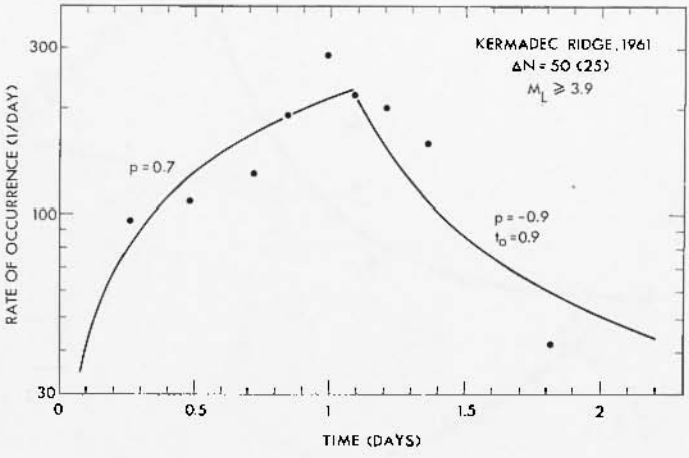

Fig. 10 – Rate of occurrence versus time, for earthquakes with $M_L \geq 4.0$, during the Kermadec Ridge swarm of 1965. Values are calculated for $\Delta N = 50$ at intervals of 25 shocks.

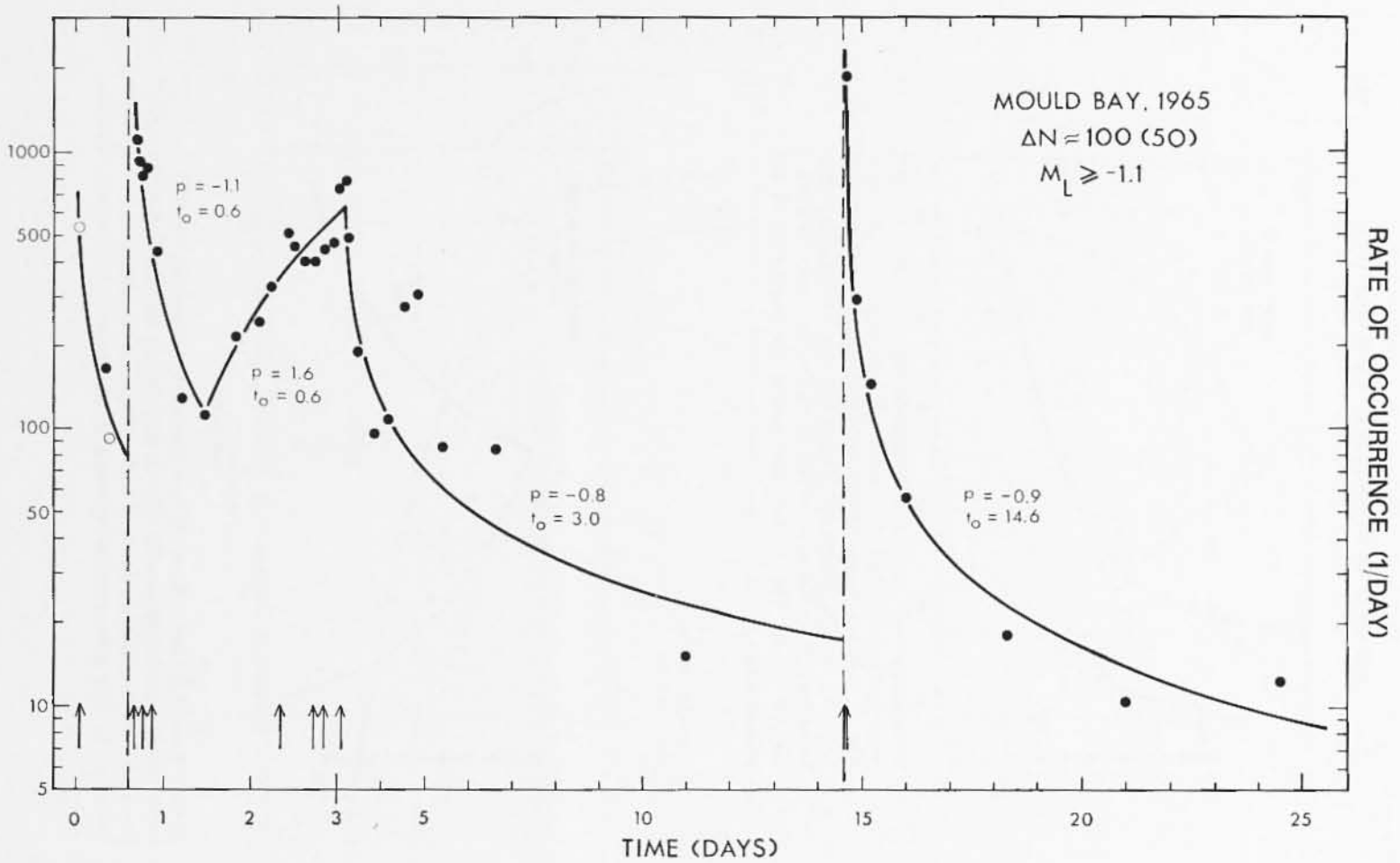

Fig. 11. – Rate of occurrence versus time, for earthquakes with $M_L \geqslant -1.1$, during the Mould Bay swarm. Values are calculated for ΔN about 100 at intervals of about 50 shocks. Open circles are for ΔN about 50. The arrowsshow earthquakes with $M_L \geqslant 2.0$.

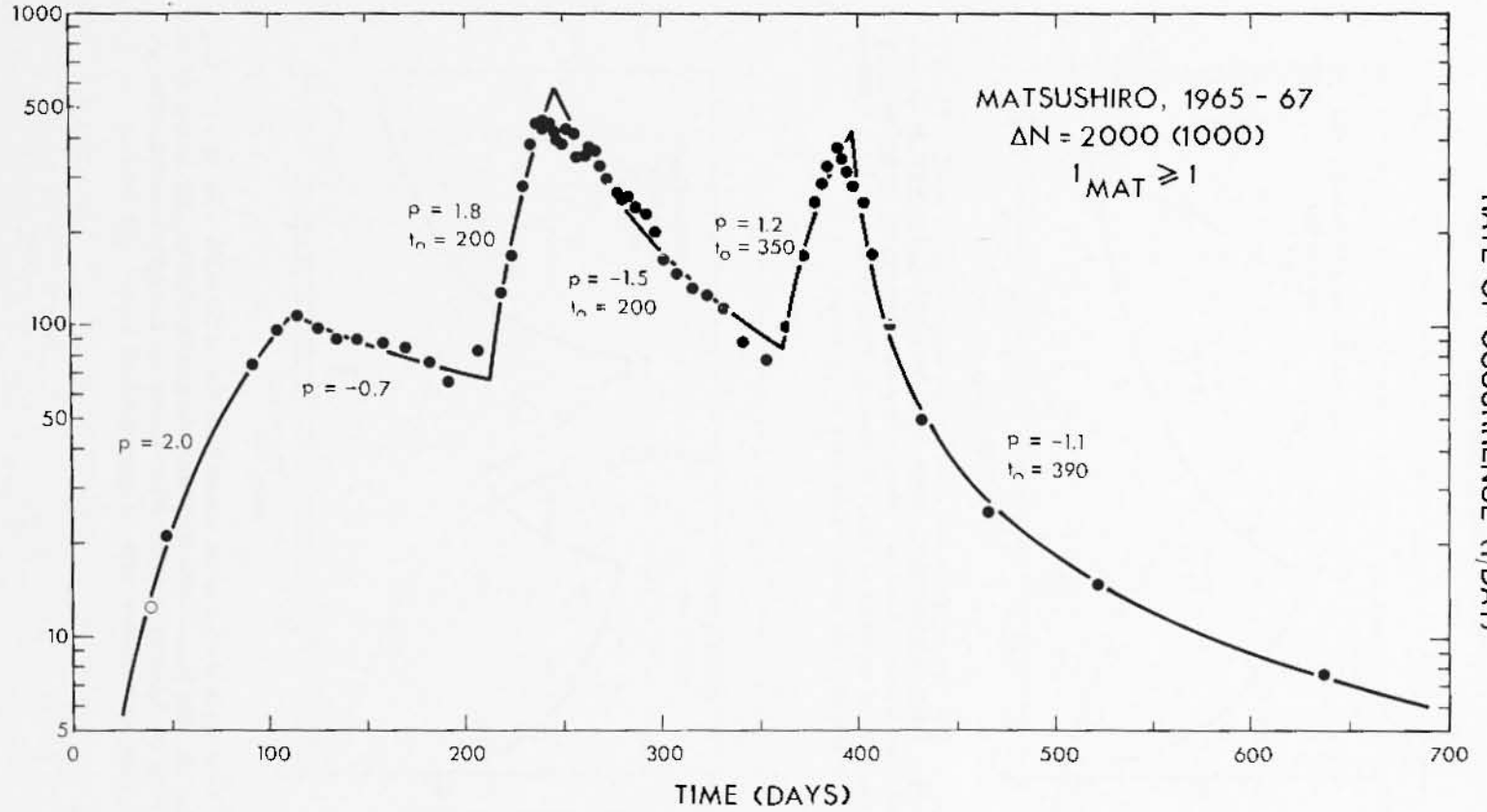

Fig. 12 – Rate of occurrence versus time, for earthquakes with $I_{MAT} \geq 1$, during the Matsushiro swarm. Values are calculated for $\Delta N = 2000$ at intervals of 1000 shocks. The first value is for $\Delta N = 1000$.

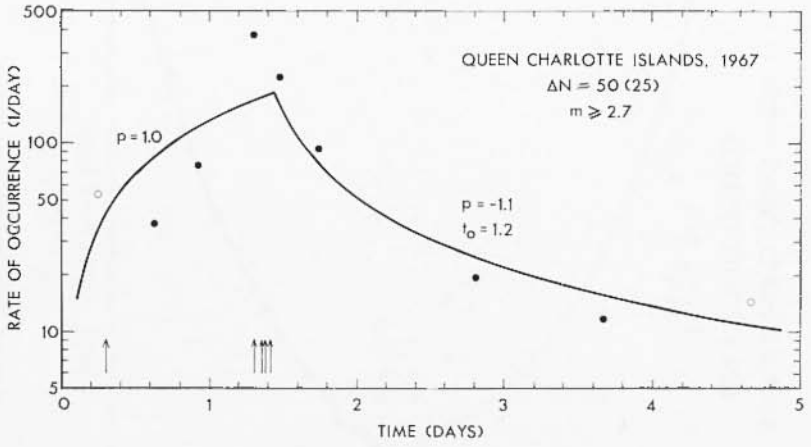

Fig. 13 – Rate of occurrence versus time, for earthquakes with $m \geq 2.7$, during the Queen Charlotte Islands swarm. Values are calculated for ΔN about 50 at intervals of about 25 shocks. Open circles are for ΔN about 25. The arrows show earthquakes with $m \geq 4\ ^1/_2$.

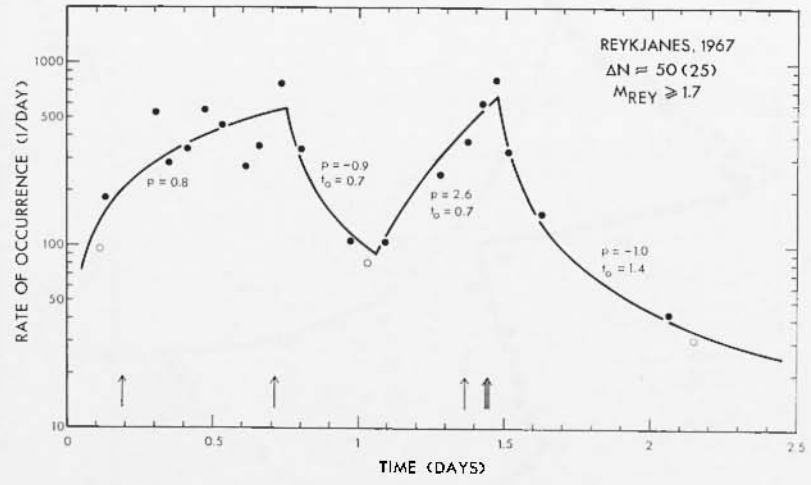

Fig. 14 – Rate of occurrence versus time, for earthquakes with $M_{REY} \geq 1.7$, during the Reykjanes swarm. Values are calculated for ΔN about 50 at intervals of about 25 shocks. Open circles are for ΔN about 25. The arrows show earthquakes with $M_{REY} \geq 4.5$.

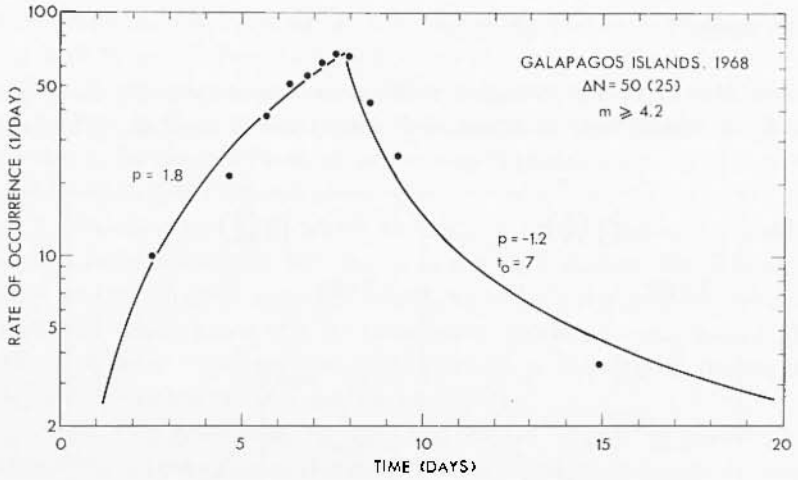

Fig. 15 – Rate of occurrence versus time, for earthquakes with $m \geq 4.2$, during the Galapagos Islands swarm. Values are calculated for $\Delta N = 50$ at intervals of 25 shocks.

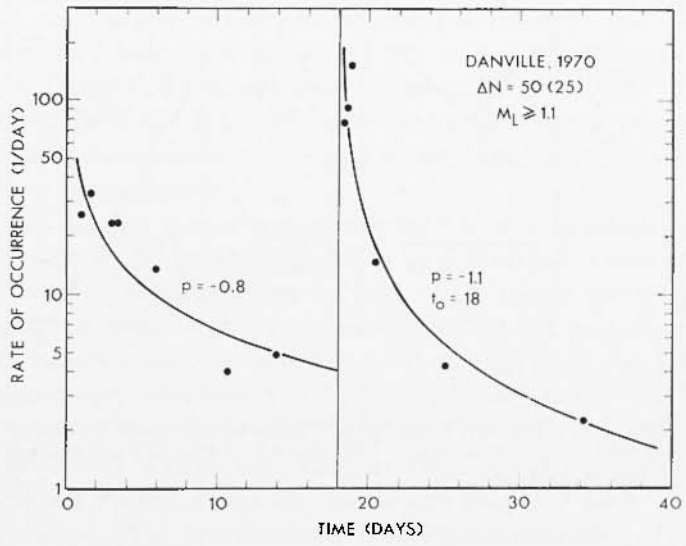

Fig. 16 – Rate of occurrence versus time, for earthquakes with $M_L \geq 1.1$, during the Danville swarm. Values are calculated for $\Delta N = 50$ at intervals of 25 shocks. The vertical line marks the beginning of the second sequences.

Discussion

Several typical patterns of earthquake swarm activity have been found, in which the variation of b with time is regular. The three

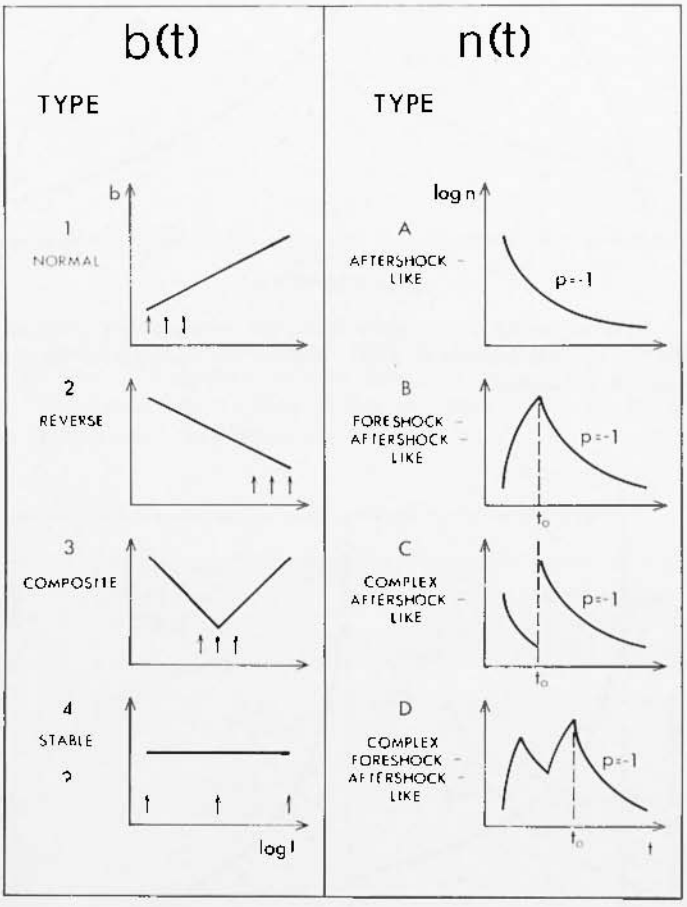

Fig. 17 — Types of earthquake swarm, classified according to $b(t)$ and $n(t)$ variations. The arrows mark the occurrence of the largest shocks.

types that can be clearly distinguished are shown schematically in Fig. 17. Since the value of b is believed to be inversely correlated with the stress in the area, the various types of swarm must have different mechanisms. In a swarm of type 1 the stress decreases after the

largest shocks, which occur at the beginning of the sequence. In a swarm of type 2 it increases, producing the largest events in the final stages. When enough stress has been released, the earthquakes stop. In a swarm of type 3, the stress increases until the release of the largest shocks in the middle of sequence, and then decreases until stability is achieved and the swarm ends.

A possible type 4, in which the rate of stress release is constant, has not been observed, but the changes in b during the Kermadec Ridge swarm of 1965 are very small, and the difference between the initial and final values of b is statistically significant only at the 75% confidence level. The reality of the changes is therefore in doubt, and this could possibly be an example of type 4.

Type 1 corresponds to the dislocation model of earthquake swarms ([26]). In this model the relative number of large shocks decreases with time, implying that the b-value increases. Teisseyre applied this type 1 model to the Matsushiro swarm, which was shown above to be of type 3. The decrease in b was observed, however, only during first 100 days of the swarm, and it has since been increasing for at least 700 days.

Table II lists the types of $b(t)$ variation for the swarms studied. Full data were available for only six of the sequences. For the Reykjanes swarm b–values are known for two stages ([28]). They are significantly different and indicate that the swarm is of type 2. For the Miyake Island, Mould Bay and Queen Charlotte Islands swarms only the time of occurrence of the largest earthquakes is known, and the allocations are tentative.

The changes of rate of occurrence with time also display several patterns (Fig. 17). A single stage, showing a decrease in rate like that in an aftershock sequence (type A), was found during two sequences. Changes of rate reminiscent of a foreshock-aftershock pattern (type B) but with more vigorous foreshock stage than that preceding a normal large earthquake, were observed during three sequences. A complex pattern (type C) showing several stages each having a decrease in rate similar to that of aftershocks, was found during two swarms. A still more complex pattern (type D), containing stages of both foreshock and aftershock type, characterizes three further swarms. These are also listed in Table II.

In all the sequences studied the decrease in rate of occurrence during the final stage was very similar to that in an aftershock sequence, with a decay coefficient close to -1.

The present data provide no evidence of any correlation between the various types of variation of $b(t)$ and the types of changes in $n(t)$. All possible combinations of types seem to be possible. A curious combination occurs in the Galapagos Islands swarm, where the b–variation was of type 1 and the largest shocks have occurred during the first 3.5 days, but the n–changes were of type B with t_0 equal to 7-8 days. Further observations of earthquakes and further microfracturing experiments on rocks are both needed if a physical explanation of the nature of various patterns is to be found.

ACKNOWLEDGMENT

I am very grateful to Mr G. A. Eiby for discussion and great assistance in preparing the text of this paper, and to Drs R. D. Adams and T. Hatherton, who also read the manuscript and made useful suggestions.

REFERENCES

(1) AKI K., 1965. – *Maximum likelihood estimate of b in the formula log N = a — b M and its confidence limits.* "Bull. Earth. Res. Inst.", **43**, 237-239.

(2) BUFE C. G., 1970. – *Frequency-magnitude variations during the 1970 Danville earthquake swarm.* "Earthq. Notes", **51**, 3, 3-7.

(3) EIBY, G. A., 1966. – *Earthquake swarms and volcanism in New Zealand.* "Bull. Volc.", **29**, 61-74.

(4) GIBOWICZ S. J., 1972. – *The relationship between telescismic body – wave magnitude m and local magnitude M_L from New Zealand earthquakes.* "Bull. Seism. Soc. Am", **62**, 1-11.

(5) GIBOWICZ S. J., 1973. – *Variation of the frequency-magnitude relation during earthquake sequences in New Zealand.* "Bull. Seism. Soc. Am.", **63**, 517-528.

(6) GIBOWICZ S. J., 1973. – *Variation of the frequency-magnitude relationship during Taupo earthquake swarm of 1964-65.* "New Zealand J. Geol. Geophys.", **16**, 18-51.

(7) GIBOWICZ S. J., 1973. – *Stress drop and aftershocks.* "Bull. Seism. Soc. Am.", **63**, 4, 1433-1446.

(8) GIBOWICZ S. J., 1973. – *Two earthquake swarms on the Kermadec Ridge.* "New Zealand J. Geol. Geophys.", submitted for publication.

(9) GUTENBERG B. and RICHTER C. F., 1954. – *Seismicity of the Earth and associated phenomena*. Princeton Univ. Press., Princeton.

(10) HAGIWARA T. and IWATA T., 1968. – *Summary of the seismographic observation of Matsushiro swarm earthquakes*. "Bull. Earthq. Res. Inst.", **46**, 485-515.

(11) ICHIKAWA M., 1969. – *Matsushiro earthquake swarm*. "Geophys. Mag.", **34**, 307-331.

(12) IWATA T., 1970. – *On the earthquake swarm in the Galapagos Islands region in June and July, 1968*. "Bull. Earthq. Res. Inst.", **48**, 935-954.

(13) KÁRNÍK V., 1969. – *Seismicity of the European area, Part 1*. D. Reidel Publish. Comp., Dordrecht.

(14) KASAHARA K. and TEISSEYRE R., 1966. – *A dislocation model of earthquake swarms*. "Bull. Earthq. Res. Inst.", **44**, 793-810.

(15) KISSLINGER C., 1968. – *Energy density and the development of the source region of the Matsushiro earthquake swarm*. "Bull. Earthq. Res. Inst.", **46**, 1207-1224.

(16) LEE W. H. K., EATON M. S. and BRABB E. E., 1971. – *The earthquake sequence near Danville, California, 1970*. "Bull. Seism. Soc. Am.", **61**, 1771-1794.

(17) MOGI K., 1963. – *Some discussions of aftershocks, foreshocks, and earthquake swarms – The fracture of a semi-infinite body caused by an inner stress origin and its relation to the earthquake phenomena* (3rd paper). "Bull. Earthq. Res. Inst.", **41**, 615-658.

(18) OIKE K., 1970. – *The time variation of the focal mechanism and the activity of earthquake swarms*. "Bull. Disas. Prev. Res. Inst. Kyoto Univ.", **19**, 4, 21-35.

(19) PAGE R., 1968. – *Aftershocks and micro-aftershocks of the great Alaskan earthquake of 1964*. "Bull. Seism. Soc. Am.", **58**, 1131-1168.

(20) RANALLI G., 1969. – *A statistical study of aftershock sequences*. "Ann. Geofisica", **XXII**, 359-397.

(21) SBAR M. L., ARMBRUSTER J. and AGGARWAL Y. P., 1972. – *The Adirondack, New York, earthquake swarm of 1971 and tectonic implications*. "Bull. Seism. Soc. Am.", **62**, 1303-1317.

(22) SCHOLZ C. H., 1968. – *The frequency-magnitude relation of microfracturing in rock and its relation to earthquakes*. "Bull. Seism. Soc. Am.", **58**, 399-415.

(23) SMITH W. E. T., WHITHAM K. and PICHÉ W. T., 1968. – *A microearthquake swarm in 1965 near Mould Bay, N.W.T., Canada*. "Bull. Seism. Soc. Am.", **58**, 1991-2011.

(24) SYKES L. R., 1970. – *Earthquake swarms and sea-floor spreading*. "J. Geophys. Res.", **75**, 6598-6611.

(25) SYLVESTER A. G., SMITH S. W. and SCHOLZ C. H., 1970. – *Earthquake swarm in the Santa Barbara Channel, California, 1968*. "Bull. Seism. Soc. Am.", **60**, 1047-1060.

([26]) TEISSEYRE R., 1970. – *Theoretical calculations of the earthquake swarm activities*, in *Symposium on earthquake physics, Warsaw, May 1969*. "Publ. Inst. Geophys. Polish Ac. Sci.", **36**, 3-13.

([27]) THATCHER W. and BRUNE J. N., 1971. – *Seismic study of an oceanic ridge earthquake swarm in the Gulf of California*. "Geophys. J. Roy. Astr. Soc.", **22**, 473-489.

([28]) TRYGGVASON E., 1970. – *Surface deformation and fault displacement associated with an earthquake swarm in Iceland*. "J. Geophys. Res.", **75**, 4407-4422.

([29]) UTSU T., 1961. – *A statistical study on the occurrence of aftershocks*. "Geophys. Mag.", **30**, 521-605.

([30]) UTSU T., 1965. – *A method for determining the value of b in a formula* $\log n = a - bM$ *showing the magnitude-frequency relation for earthquakes*. "Geophys. Bull. Hokkaido Univ.", **13**, 99-103.

([31]) UTSU T., 1966. – *A statistical significance test of the difference in b-value between two earthquake groups*. "J. Phys. Earth", **14**, 2, 37-40.

([32]) WARD P. L. and BJORNSSON S., 1971. – *Microearthquakes, swarms, and the geothermal areas in Iceland*. "J. Geophys. Res.", **76**, 3953-3982.

([33]) WARREN N. W. ad LATHAM G. V., 1970. – *An esperimental study of thermally induced microfracturing and its relation to volcanic seismicity*. "J. Geophys. Res.", **75**, 4455-4464.

([34]) WESTMILLER R. J., 1971. – *An earthquake swarm on the Queen Charlotte Islands Fracture Zone*. "Bull. Seism. Soc. Am.", **61**, 1489-1505.

([35]) WYSS M., 1973. – *Towards a physical understanding of the earthquake frequency distribution*. "Geophys. J. Roy. Astr. Soc.", **31**, 341-359.